



Contents lists available at ScienceDirect

Biologicals

journal homepage: [www.elsevier.com/locate/biologicals](http://www.elsevier.com/locate/biologicals)

## Is *Pichia pastoris* a realistic platform for industrial production of recombinant human interferon gamma?

Ali Razaghi<sup>a, b</sup>, Emilyn Tan<sup>c</sup>, Linda H.L. Lua<sup>c</sup>, Leigh Owens<sup>d</sup>, O.P. Karthikeyan<sup>e</sup>,  
Kirsten Heimann<sup>a, b, \*</sup>

<sup>a</sup> College of Science and Engineering, James Cook University, Townsville 4811, Qld, Australia

<sup>b</sup> Centre for Biodiscovery and Molecular Development of Therapeutics, James Cook University, Townsville 4811, Qld, Australia

<sup>c</sup> The University of Queensland, Protein Expression Facility, Brisbane 4072, Qld, Australia

<sup>d</sup> College of Public Health, Medical and Veterinary Science, James Cook University, Townsville 4811, Qld, Australia

<sup>e</sup> Department of Biology, Hong Kong Baptist University, Hong Kong

### ARTICLE INFO

#### Article history:

Received 18 July 2016

Received in revised form

30 August 2016

Accepted 29 September 2016

Available online xxx

#### Keywords:

Biopharmaceuticals

*Pichia pastoris*

Protein expression

Interferon gamma

Low-abundance RNA

Minimum free energy

### ABSTRACT

Human interferon gamma (hIFN $\gamma$ ) is an important cytokine in the innate and adaptive immune system, produced commercially in *Escherichia coli*. Efficient expression of hIFN $\gamma$  has been reported once for *Pichia pastoris* (Wang et al., 2014) – a proven heterologous expression system. This study investigated hIFN $\gamma$  expression in *P. pastoris* replicating the previous study and expanding by using four different strains (X33: wild type; GS115: HIS<sup>-</sup>Mut<sup>+</sup>; KM71H: Arg<sup>+</sup>, Mut<sup>-</sup> and CBS7435: Mut<sup>S</sup>) and three different vectors (pPICZ $\alpha$ A, pPIC9 and pPpT4 $\alpha$ S). In addition, the native sequence (NS) and two codon-optimised sequences (COS1 and COS2) for *P. pastoris* were used. Methanol induction yielded no expression/secretion of hIFN $\gamma$  in X33, highest levels were recorded for CBS7435: Mut<sup>S</sup> (~16  $\mu$ g. L<sup>-1</sup>). mRNA copy number calculations acquired from RT-qPCR for GS115-pPIC9-COS1 proved low abundance of mRNA. A 10-fold increase in expression of hIFN $\gamma$  was achieved by lowering the minimal free energy of the mRNA and 100-fold by Mut<sup>S</sup> phenotypes, substantially lower than reported by Wang et al. (2014). We conclude that commercial production of low cost, eukaryotic recombinant hIFN $\gamma$  is not an economically viable in *P. pastoris*. Further research is required to unravel the cause of low expression in *P. pastoris* to achieve economic viability.

© 2016 International Alliance for Biological Standardization. Published by Elsevier Ltd. All rights reserved.

### 1. Introduction

Natural human interferon gamma (hIFN $\gamma$ ) is a glycoprotein comprised of 166 amino acids including a secretory signal sequence of 23 amino acids, encoded by a single gene on chromosome 12 [1,2]. hIFN $\gamma$  is classed a cytokine with miscellaneous functions in the regulation of innate and adaptive immune system responses. It has been reported to be an immuno-modulatory clinically effective drug due to its pleiotropic effects against a wide range of diseases like cancers, hepatitis and tuberculosis [3].

To date, commercial production of recombinant hIFN $\gamma$  is limited to expression in *E. coli*, which is branded as Actimmune<sup>®</sup> and approved by the US-Food & Drug Administration, (FDA) for the

treatment of chronic granulomatous disease and severe malignant osteopetrosis [1,2]. This recombinant form of hIFN $\gamma$  is an unglycosylated monomer composed of 143 amino acids, rendering it less protease-resistant, resulting in a shorter half-life in the bloodstream compared to the glycosylated form [1–3]. Other drawbacks associated with *E. coli* expression systems include: potential for endotoxin contamination and the formation of intracellular protein aggregates, termed inclusion bodies, requiring a complex purification and protein refolding process. This increases the final cost of the product [3].

To overcome these limitations, expression of recombinant hIFN $\gamma$  was attempted in various hosts like *Saccharomyces cerevisiae* 20B-12 [4], insect cells lines *Spodoptera frugiperda*, *Spodoptera exigua*, and *Spodoptera litura*. [5], Chinese hamster ovary (CHO) [3,6], wild-type mice strain C57BL/6 [7], rat cell line 3Y1-B [8], monkey and human cells [9]; however; high costs of cultivation and purification, contamination, low yields, low biological activity and short half-life of the product also adversely impacted on the use of these expression systems [10].

\* Corresponding author. College of Science and Engineering, James Cook University, Townsville 4811, Qld, Australia. Fax: +61 7 4725 1570.

E-mail address: [Kirsten.heimann@jcu.edu.au](mailto:Kirsten.heimann@jcu.edu.au) (K. Heimann).

### Abbreviations

AGRF	Australian Genome Research Facility
AOX	alcohol oxidase
BMGY	buffered glycerol complex medium
BMMY	buffered methanol complex medium
CHO	Chinese hamster ovary
COS1	codon-optimised sequence 1
COS2	codon-optimised sequence 2
GOI	gene of interest
hIFN $\gamma$	human interferon gamma
HPLC	high pressure liquid chromatography
MFE	minimum free energy
MGY	minimal glycerol medium
MM	minimal methanol medium
NS	native sequence
T <sub>m</sub>	melting temperature
YNB	yeast nitrogen base

Another yeast-based expression system for recombinant hIFN $\gamma$  is the methylotrophic yeast, *Pichia pastoris* (synonym. *Komagataella pastoris*), a proven successful heterologous expression system for the production of hundreds of recombinant proteins [11]. The *P. pastoris* expression systems offer distinct advantages such as easy manipulation, high cell densities, cultivation in low acidity reducing the chance of contamination, low cost of production, eukaryotic post-translational modification and secretion, including protein folding and glycosylation [11].

Commercially available *P. pastoris* strains are the auxotrophic strains GS115 (the *HIS4* mutant), KM71H (the *AOX1* and *ARG4* mutant), the reconstituted prototrophic strain X-33 and protease-deficient strains such as SMD1168. However, use of these strains for commercial applications is restricted by intellectual property [11]. In contrast, some strains of *P. pastoris* like CBS7435, are not protected by patent and, thus represent an alternative for production purposes [11].

The most commonly used promoter capable of driving recombinant protein expression in *P. pastoris*, is the strong alcohol oxidase (*AOX*) promoter which is only inducible with methanol [12]. Two *AOX* operons can be found in the *P. pastoris* chromosome: *AOX1* is responsible for the major *AOX* activity, and *AOX2*, which plays a minor role [12]. Recombinant gene techniques for transformation of *P. pastoris* can leave either or both *AOX* gene sets functional, only the *AOX2*, or neither. Thus, the resulting phenotypes are referred to as Mut<sup>+</sup> (methanol utilisation plus), Mut<sup>S</sup> (methanol utilisation slow), or Mut<sup>-</sup> (methanol utilisation minus), respectively. Expression efficiency for a recombinant protein in a particular recombinant is not predictable, and available information is at odds in this respect [12].

This study was based on the study by Wang et al. (2014) using native and *P. pastoris* codon-optimised sequences of hIFN $\gamma$  and expanded the study using eight combinations of *P. pastoris* strains, vectors and sequences. Surprisingly, expression were orders of magnitudes lower than previously reported [10]. Based on our low expression/secretion results for all constructs and in agreement with very recently published results [13], we conclude that the *P. pastoris* expression/secretion system is at present not economically viable for commercial production of eukaryotic recombinant hIFN $\gamma$  (Animation 1).

Supplementary video related to this article can be found at <http://dx.doi.org/10.1016/j.biologicals.2016.09.015>.

## 2. Material and methods

### 2.1. Strains, sequences, vectors and cloning

#### 2.1.1. Strains

Four strains of *P. pastoris* with different characteristics were used; **X33**: wild-type strain containing two active *AOX* genes resulting in Mut<sup>+</sup> phenotype, **GS115**: A His<sup>-</sup> mutant (mutation of *HIS4*), with the His<sup>-</sup> Mut<sup>+</sup> phenotypes, **KM71H**: A mutant strain with *ARG4* (arginosuccinate lyase) and disruption of *AOX1*, creating a Mut<sup>S</sup> Arg<sup>+</sup> phenotype, **CBS7435**, **Mut<sup>S</sup>**: a knockout of the *AOX1* gene derived from the wild-type CBS7435 strain.

#### 2.1.2. Sequences

In this study, two distinct codon-optimised sequences of hIFN $\gamma$  were synthesised based on the codon preference of *P. pastoris* by Invitrogen™, GeneArt™ Strings, and one copy of the native sequence of hIFN $\gamma$  “NCBI: NM\_000610.2; UniProtKB: P01579” was used as a positive control (Fig. 1).

#### 2.1.3. Vectors

The vectors used in this study for transformation of *P. pastoris* are shown in (Fig. 2). **pPIC9**: was provided by Invitrogen™ (catalogue no. K1710-01). This plasmid contains a methanol-inducible *AOX1* promoter, the  $\alpha$ -mating secretion signal at the 5' end of the gene of interest (GOI) and the *HIS4* gene for selection enabling the GS115 strain to biosynthesise histidine. The sequence of the GOI was inserted at *NotI* and *EcoRI* restriction sites. Then, the construct was linearized using *Sall* restriction endonuclease prior to transformation. **pPICZ $\alpha$ A**: was provided by Invitrogen™ (catalogue no. K1710-01). This plasmid contains a methanol-inducible *AOX1* promoter, the  $\alpha$ -mating secretion signal and a polyhistidine tag (*HIS*-tag) at 5' and 3' ends of the GOI, respectively. The Zeocin™ resistance gene (*Sh ble*) is placed in the plasmid which allows selection of successful transformants on Zeocin™ containing medium plates. The sequence of the GOI was inserted at *EcoRI* and *NotI* restriction sites. Then, 5  $\mu$ g of the construct was linearized using *SacI* restriction endonuclease prior to transformation. **pPpT4 $\alpha$ S**: was provided by Protein Expression Facility at The University of Queensland (Brisbane, Australia). This plasmid contains the methanol-inducible *AOX1* promoter and the  $\alpha$ -mating secretion signal at the 5' end of the GOI. The Zeocin™ resistance gene (*Sh ble*) was placed in the plasmid which allows selection of successful transformants on Zeocin™ containing medium plates [14]. The native secretion signal was omitted from the sequence of the GOI followed by insertion at *SnaBI* and *NotI* restriction sites. Then, 5  $\mu$ g of the construct was linearized using *SwaI* restriction endonuclease prior to transformation.

Gene sequences in vectors (pPICZ $\alpha$ A and pPpT4 $\alpha$ S) were verified by using ABI BigDye Terminator v3.1 sequencing, conducted by the Australian Genome Research Facility (AGRF). Data analysis was performed using the software Sequencer™ 4.7 (Gene Codes Corporation).

<sup>1</sup> In this study, several codon-optimised sequences were designed for *P. pastoris* based on codon preference. COS1 was selected according to similarity of GC% and T<sub>m</sub> to the NS. Upon review, RNA truncation due to polyadenylation (poly A) signals appeared possible. COS2 was designed by replacing putative poly A signals (bases 292–297, 331–338 and 457–466) and lowering the predicted minimum free energy (MFE) of the mRNA compared to COS1 (Section 2.8).

```

NS      ATGAAATACAAAGTTATATCTTGGCTTTTCAGCTCTGCATCGTTTGGGTCTCTTGGC
COS1   ATGAAGTACACATCTACATCTTGGCTTTCCAGTTGTGTATCGTTTGGGTCTCTTGGC
COS2   ATGAAATACACCTTATATATACTTGCCTCCAGTTATGCATTTGTTGGTGTCTGGGG
*****

NS      TGTACTGCCAGGACCATATGTAAGGAAAGCAGAAAACCTTAAGAAATTTTAAATGCA
COS1   TGTACTGTCAAGGACCATACGTTAAGGAAAGCTGAGAACTTGAAGAAGTACTTCAACGCT
COS2   TGTATTGCCAAGTCCATATGTGAAAGAAAGCCGAAAACCTGAAAAGTACTTCAACGCC
*****

NS      GGTCACTCAGATGATAGCGGATATGGAAGTCTTTTCTTAGGCATTTTGAAGAATTGAAAA
COS1   GGTCACTCCGAGTTGCTGATAACGGTACTTTGTTCTGGGTATCTTGAAGAAGTGGAAA
COS2   GGACATAGTATGATGTCAGACAAACGGCACACTATTTCTGGTATTCTAAGAAGTGGAA
*****

NS      GAGGAGATGACAGAAAAAATGACAGAGCAAATGTCTCTTTTACTTCAAACCTTTT
COS1   GAAGAGTCCGACAGAAAGATCATGAGTCCAGATCGTTTCATTCTACTTCAAGTGTGTC
COS2   GAGGAGTCTGACCGTAAATTTATGCAATCAAAATCGTTTCTTTTACTTAAACATTC
*****

NS      AAAAAGTAAAGATGACCAAGATCCAAAAGAGTGTGGAGACCATCAAGGAAGACATG
COS1   AAGAACTTCAAGGACGACAGTCCATCCAGAAAGTCCGTTGAGACTATCAAGGAAGATATG
COS2   AAAAATTTAAAGATGACCAATCAATCAAAAGAAAGAGGAGGACGATTAAGAAAGATG
*****

NS      AATGTCAAGTTTTTCAATAGCAACAAAAGAAAGAGAGTACTTCAAGAAAGTACTAAT
COS1   AAGCTTAAAGTTCTTCACTTCAACCAAGAAAAGAGAGAGTACTTCAAGAAAGTACTAAT
COS2   AATGTCAAGTTTTTCACTTCAACCAAAAAGAAAGAGGAGGACGATTTGAAAAGTAACTAAT
*****

NS      TATTCGGTAACTGACTTGAATGTCCAACGAAAGCAATACATGAAGTCTCAAGTGATG
COS1   TACTCCGTACTGACTTGAACGTTCAAGAAAAGGCTATCCAGAGTTGATCCAGGTTATG
COS2   TATTCGGTAACTGACTTGAACGTTCAAGAAAAGGCAATCCATGAGTTGATCAAGGTTATG
*****

NS      GCTGAAGTGTGCGCAGCAGTAAAACAGGGAAGCGAAAAGGAGTCAAGTGTGTTTCCGA
COS1   GCTGAATGTCTCCAGCTGCTAAGACTGTTAAGGAAAAGATCCAGAGTGTGTTTCCAGA
COS2   GCGAAGTGTGTTTCCAGCTGCTAAGACTGTTAAGGAAAAGGAGGAGGATCAAAATGCTTTCCAG
*****

NS      GGTCAAGAGCATCCCAAGTAA
COS1   GGTAGAAGACTTCCCAAGTAA
COS2   GGTAGACGTCTTCAAGTAA
*****

POI    MQDPYVKEAENLKKYFNAGHSDVADNGLFLGILKNNKEESDRKIMQSQIVSYFYKLFKN
      FKDDQSIQKSVETIKEDMNVKFFNSNKKRDFELKTNYSVDLNVQRKAIHELQVMAE
      LSPAATGKRRKRSQMLFRGRASQ

```

**Fig. 1.** DNA sequences of *hIFN $\gamma$* ; **NS**: Native sequence, **COS1**: Codon-optimised sequence 1, **COS2**: Codon-optimised sequence 2. **POI**: Protein of interest i.e. amino acid sequence of *hIFN $\gamma$* . (\*): Presence of this symbol shows the similarity in the bases. The first 23 amino acid sequence (eq. 69 bp nucleotides) is the native secretion signal at the N-terminal of the amino acid sequence.

## 2.2. Transformation into *Pichia pastoris*

### 2.2.1. Order of transformation

In order to generate the construct; each sequence was flanked with suitable restriction enzymes listed in (Fig. 2) and inserted into the vectors between the same restriction sites. Prior to transformation, each construct was linearized using suitable restriction enzymes for the vector (Fig. 2). The combinational order for generating each transformant is listed in (Table 1).

### 2.2.2. Electroporation of *Pichia pastoris*

Each plasmid pPIC9-COS1 & pPIC9-COS2 was linearized with suitable corresponding restriction enzymes (Fig. 2) and then transformed into the *P. pastoris* GS115 strain by electroporation (Electroporator 2510™, Eppendorf) following the protocols for electro-competent cell production and electroporation (Invitrogen™).

Each plasmid pPIC $\alpha$ -NS, pPIC $\alpha$ -COS2, pPpT4 $\alpha$ S-NS, pPpT4 $\alpha$ S-COS2, were linearized with suitable corresponding restriction enzymes (Fig. 2) and then transformed into either X33, KM71H or CBS7435 strains of *P. pastoris* by electroporation (Electroporator Thermo Hybaid Cellject Pro®, ADP-400) following the protocols for electro-competent cell production and electroporation [15].

### 2.2.3. Screening for transformants

pPIC9-COS1 & pPIC9-COS2-transformed GS115 (Table 1) were screened for HIS<sup>+</sup> phenotype on Minimal Dextrose (MD) (1.34% Yeast Nitrogen Base (YNB), 2% dextrose) agar plates in 30 °C, as successful transformants should have regained histidine auxotrophy. With the intention of determining the methanol utilisation (Mut) phenotype of the strain, colonies with HIS<sup>+</sup> phenotype were re-plated on Minimal Methanol (MM) (1.34% YNB, 0.5% methanol) as the sole carbon source, the methanol utilisation plus (Mut<sup>+</sup>) phenotype was chosen by the ability to grow on both media agar plates after 24 h while methanol utilisation slow (Mut<sup>S</sup>) cells grow normally on MD, but their growth on MM was negligible.

The remainder of the transformants which were obtained from other strains of *P. pastoris* i.e. X33, KM71H and CBS7435 (Table 1) were selected by plating onto selective medium (1% Yeast 2% Peptone 1% Dextrose plus Zeocin™ 100  $\mu$ g mL<sup>-1</sup>) after 5 days' incubation at 30 °C.

### 2.2.4. Confirmation of integration into gDNA by PCR

In order to determine, whether *hIFN $\gamma$*  was integrated into the *P. pastoris* genome, colony PCR was conducted for X33, KM71H and CBS7435 transformants, while genomic DNA was extracted from GS115 transformants using the Wizard® Genomic DNA Purification Kit, (Promega) for PCR. The integration of *hIFN $\gamma$*  into the genome of *P. pastoris* was confirmed by PCR using primers listed in Table 2. Genomic DNA of untransformed *P. pastoris* strains was used as a negative control. PCR amplification was run according to the standard protocol for *P. pastoris* (Invitrogen™).

Successful integration of *hIFN $\gamma$*  into *P. pastoris* genome was demonstrated by detecting the expected ~500–800 bp fragment size using agarose (1.5%) gel electrophoresis.

## 2.3. Expression of *hIFN $\gamma$*

### 2.3.1. Standard expression in *P. pastoris* in buffered medium

Transformant cells (GS115-pPIC9-COS1 and GS115-pPIC9-COS2) were cultivated in 25 mL buffered Minimal Glycerol (BMGY) medium (1.34% YNB, 1% glycerol, 100 mM potassium phosphate, pH 6.0) in a 250 mL baffled flask and incubated for 48 h at 28 °C on a shaking plate at 200 rpm until reaching an OD<sub>600</sub>  $\geq$  2 (log-phase growth) (EnSpire® Multimode Plate Reader, PerkinElmer). Next, the cells were harvested by centrifugation for 5 min at 3000 g at room temperature. Then, cell pellets were resuspended in 50 mL PBS buffer (0.1 M Phosphate Buffer Saline, pH 7.4) to wash off residual glycerol. Finally, cell pellets were resuspended in 50 mL buffered methanol-complex (BMMY) medium (2% peptone, 1% yeast extract, 1.34% YNB, 1% methanol, 100 mM potassium phosphate, pH 6.0) to a starting OD<sub>600</sub> = 1 in a 250 mL baffled flask. Methanol was added to a final concentration of 1% (v/v) every 24 h to induce expression of *hIFN $\gamma$* . The culture supernatant was obtained after 72 h of cultivation by centrifugation at 1500 g for 5 min to analyse the expression of *hIFN $\gamma$* , untransformed *P. pastoris* GS115 cell culture was used as negative control [16].

### 2.3.2. High throughput expression in *P. pastoris* in buffered medium

Small-scale expression screens were performed in 24 deep-well plates for the transformant strains of X33, KM71H and CBS7435. It was shown that oxygenation for the deep well plates used was comparable to levels achieved in baffled flasks [17]. Following inoculation of 5 mL BMGY media with a single colony, cultures were grown at 30 °C with shaking at 250 rpm for 48 h. Then, the BMGY media was removed by centrifugation at 1000 g for 10 min and each cell pellet was washed with 4 mL of PBS twice. After the second wash, the cell pellets were resuspended in 5 mL of BMMY medium to induce expression. Methanol was added to 1% (v/v) every 24 h until harvest. Samples were harvested 96-h post-induction (hpi) for

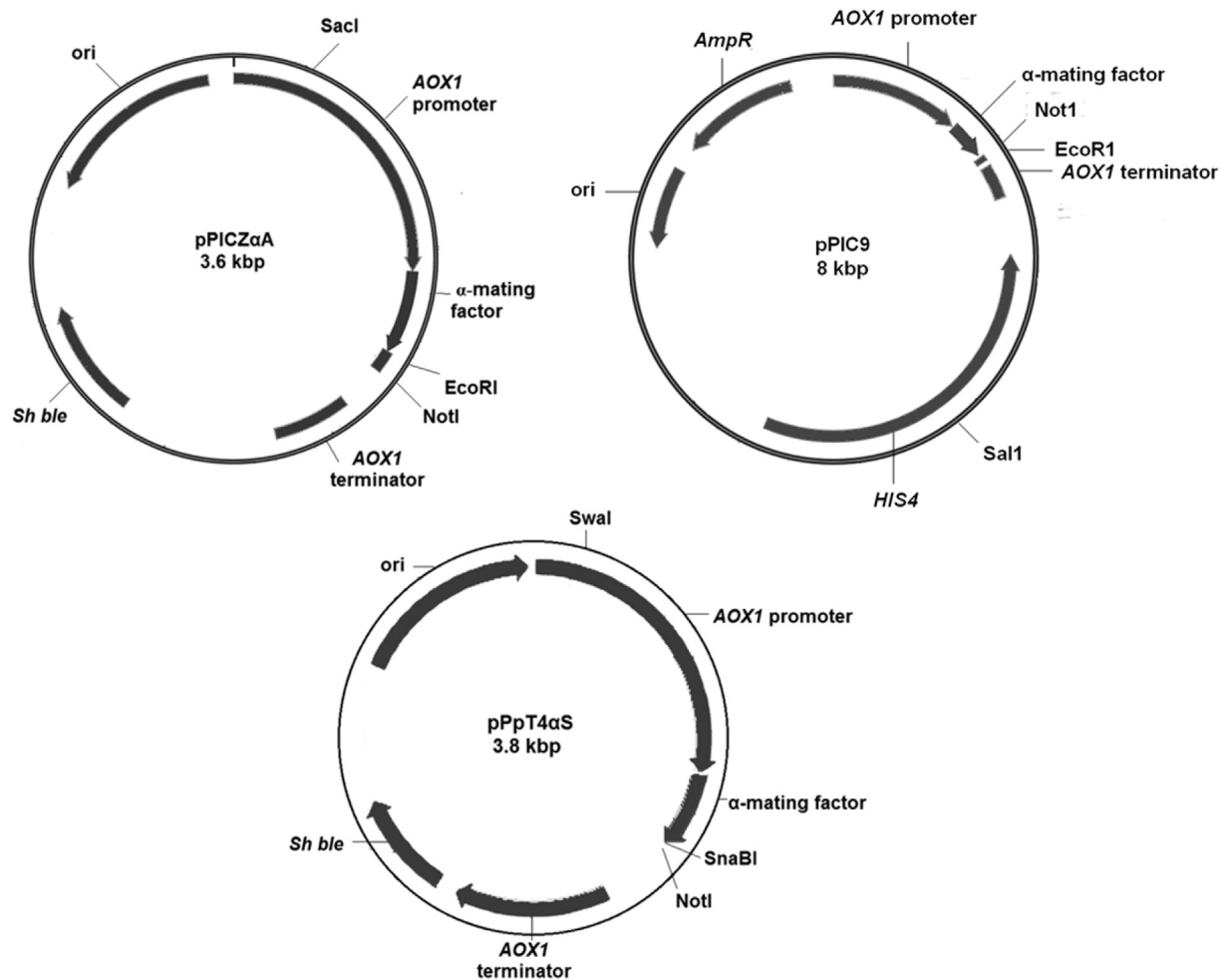


**Fig. 2.** Generic plasmid vector maps of pPIC9, pPICZ $\alpha$ A, pPpT4 $\alpha$ S. **Ori**: the origin of replication, for more information consult the text. **6His-tag**: polyhistidine tag. **Sh ble**: The Zeocin™ resistance gene **AOX**: alcohol oxidase gene.

analysis. Untransformed strains of X33 (Mut<sup>+</sup>), CBS7435 (Mut<sup>S</sup>) and KM71H (Mut<sup>S</sup>) were used as negative controls and a positive control (P-Protein) was cultured along with the test clones.

### 2.3.3. Expression in *P. pastoris* in unbuffered medium

There are some recombinant proteins susceptible to proteases after secretion into the culture medium. In this case, it is usually possible to use unbuffered media such as Minimal Glycerol Medium (MGY) (1.34% YNB and 1% glycerol) and Minimal Methanol (MM) (1.34% YNB and 1% methanol) to inactivate secreted proteases, as the pH drops to 3 or below during cultivation, inactivating many proteases, while *P. pastoris* is tolerant to the acidic condition [18]

Expression was performed in unbuffered MGY/MM instead of BMGY/BMMY following the same protocol as detailed in 2.3.1.

### 2.4. Cell lysis for protein extraction

A modified version of the standard cell lysis technique for *P. pastoris* was used (Invitrogen™) following this procedure; 1 mL of culture (as detailed in 2.3.1) was centrifuged for 5 min at 3000 g to remove the supernatant then washed once in Breaking Buffer (50 mM sodium phosphate, pH 7.4, 1 mM EDTA, 5% glycerol plus 1 dissolved tablet of Sigma FAST™ Protease Inhibitor Cocktail Tablet #S8830 in 100 mL of distilled water) by resuspension and

**Table 1**

Combinational order of expression systems, strains, vectors and sequences which have been used for cloning and transformation.

Expression system	Strain	Vector	Sequence of GOI	Transformant	Phenotype
<i>Pichia pastoris</i>	GS115	pPIC9	COS1	GS115-pPIC9-COS1	His <sup>+</sup> Mut <sup>+</sup>
			COS2	GS115-pPIC9-COS2	
	X33	pPICZ $\alpha$ A	NS	X33-pPICZ $\alpha$ A-NS	Mut <sup>+</sup>
			COS2	X33-pPICZ $\alpha$ A-COS2	
	KM71H	pPpT4 $\alpha$ S	COS2	X33-pPpT4 $\alpha$ S-COS2	Mut <sup>+</sup>
			NS	KM71H-pPICZ $\alpha$ A-NS	Mut <sup>S</sup>
	CBS7435	pPICZ $\alpha$ A	COS2	KM71H-pPICZ $\alpha$ A-COS2	
			COS2	CBS7435-pPpT4 $\alpha$ S-COS2	Mut <sup>S</sup>

NS: Natural sequence, COS1: Codon-optimised sequence 1, COS2: Codon-optimised sequence 2.

**Table 2**

Primer sequences for each vector and their hybridising points on the target DNA.

Transformant	Primer sequence	Hybridising point
GS115-pPIC9-COS1/COS2	Forward	5'TACTATTGCCAGCATTTGCTGC3'
	Reverse	5'GCAATGGCATTCTGACATCC3'
X33-pPICZα-NS	Forward	5'GAGAAAAGAGAGGCTGAAGCTCAGGACCCATATGTAAGAAGC3'
	Reverse	5'GTTCTAGAAAGCTGGCGCCTTAATGATGATGGTGGTGATGCTGGGATGCTCTTCGACCT3'
X33-pPICZα-COS2	Forward	5'GAGAAAAGAGAGGCTGAAGCTCAAGATCCATATGTCAAAGAAGC3'
	Reverse	5'TTCTAGAAAGCTGGCGCCTTAATGATGATGGTGGTGATGCTGAGAAGCTCTTCTACCTC3'
X33-pPpT4αS-COS2	Forward	5'GACTGGTTCCAATTGACAAGC3'
	Reverse	5'GGCATTCTGACATCCTTGTGATTACTGAGAAGCTCTTCTACCTC3'
KM71H-pPICZα-NS	Forward	5'GACTGGTTCCAATTGACAAGC3'
	Reverse	5'GTTCTAGAAAGCTGGCGCCTTAATGATGATGGTGGTGATGCTGGGATGCTCTTCGACCT3'
KM71H-pPICZα-COS2	Forward	5'GAGAAAAGAGAGGCTGAAGCTCAAGATCCATATGTCAAAGAAGC3'
	Reverse	5'TTCTAGAAAGCTGGCGCCTTAATGATGATGGTGGTGATGCTGAGAAGCTCTTCTACCTC3'
CB7435-pPpT4αS-COS2	Forward	5'GAAGAGAGAGCGGCAAGCTCATCACCACCATCATCAAGATCCATATGTCAAAGAAGC3'
	Reverse	5'CCCAAACCCCTACCACAA3'

**GOI:** gene of interest (i.e. *hIFN $\gamma$* ), **AOX1 TT:** AOX transcription terminator.

centrifugation at 3000 g at 4 °C for 5 min. Cells were resuspended in 1 mL of Breaking Buffer and an equal volume of acid-washed glass beads was added, the mixture was vortexed for 30 s, then incubated on ice for 30 s, which was repeated 7 times. The sample was centrifuged at 4 °C for 5 min at 12,000 g and *hIFN $\gamma$*  was quantified by ELISA of the cleared supernatants. Cell lysates of untransformed *P. pastoris* GS115 were used as negative controls.

### 2.5. SDS-PAGE and western blotting

Sample supernatants were loaded on 4–12% Bis-Tris SDS-PAGE under denatured and reduced conditions (using NuPAGE<sup>®</sup> LDS sample buffer, catalogue no. NP0007). Novex<sup>®</sup> Sharp Pre-Stained Protein Standard (Catalogue no: LC5800, ThermoFisher<sup>™</sup>) was used as molecular weight ladder ranging 3.5–260 kDa. Gels were blotted to PVDF membrane and probed with the polyhistidine-HRP conjugated antibody (Miltenyi Biotec, catalogue no. 130-092-785, Lot# 5141126111) at a dilution of 1: 6000. The analysis was performed using a Bio-Rad Chemi-Doc<sup>™</sup> XRS + imaging system and the molecular weight was calculated using ProtParam.

### 2.6. ELISA

Recombinant *hIFN $\gamma$*  protein levels were quantified by indirect ELISA. A standard curve  $0, 1.25, 2.5, 5, 10, 20 \mu\text{g L}^{-1}$  ( $R^2 = 0.9904$  and  $y = 13.981x - 1.7371$ ) was prepared by serial dilution of the recombinant *hIFN $\gamma$*  (Abcam catalogue no. ab51240) [16].

(18) primers for priming cDNA synthesis; using the poly-A tail found at the 3' end of the eukaryotic mRNAs that ensures the 3' end of mRNAs is represented, and random hexamer primers which randomly cover all regions of the RNA to create a cDNA pool. The synthesised cDNA was divided into equal triplicates for treatment with the QuantiTect SYBR<sup>®</sup> Green PCR Kit (Qiagen catalogue no. 204141) for the two-step reverse transcription-PCR (RT-qPCR; determining copy number of mRNA transcript) using primers forward 5'ACTTCAACGCTGGTCACTC 3' and reverse 5' CGGACTCTG-GATGGACTG 3' to amplify 168 bp amplicon close to the 5' end of the COS1 *hIFN $\gamma$*  sequence [16].

Standard curves for qPCR were prepared with purified DNA amplicons of 699 bp of which 501 bp belong to the *hIFN $\gamma$*  gene (Section 2.2.4). Dilution series of DNA amplicons according to copy number (n/per total volume of reaction) were used to prepare standard curve with  $0, 1.33 \times 10^2, 1.33 \times 10^3, 1.33 \times 10^4$  and  $1.33 \times 10^5$  copy number ( $R^2 = 0.998$ , Overall efficiency = 101% and  $y = 10^9 \cdot e^{-0.699x}$ ).

Each 50  $\mu\text{L}$  reactions contained 25  $\mu\text{L}$  (2 $\times$ ) QuantiTect SYBR<sup>®</sup> GreenPCR Master Mix, 10  $\mu\text{M}$  forward and reverse primers with final concentrations of 0.3  $\mu\text{M}$  (5  $\mu\text{L}$  each), 6  $\mu\text{L}$  sample (~2  $\mu\text{g}$  cDNA quantified by NanoDrop<sup>®</sup>, ND-1000 Spectrophotometer) and 9  $\mu\text{L}$  RNase-free water. qPCR reactions were run on a Peltier Thermal Cycler-200 (BioRad) as per [16] Total RNA of untransformed *P. pastoris* GS115 was used as a negative control.

Approximate copy number of *hIFN $\gamma$*  mRNA transcripts per cell were calculated as per Equation (1) (Eq. (1));

$$\text{Approx. } hIFN\gamma \text{ mRNA transcript} \left( \frac{\text{Copy number}}{\text{Cell number per batch of reaction}} \right) \approx \text{Determined copy number of transcripts per volume of reaction} / 16.66 \times 10^3 \quad (1)$$

### 2.7. Detection and determination of mRNA copy number by RT-qPCR

PureLink<sup>®</sup> RNA Mini Kit (Life Technologies<sup>™</sup> catalogue no. 12183018A) was used for extraction of total RNA equivalent to  $\sim 16.66 \times 10^3$  amount of yeast cells (GS115-pPIC9-COS1), followed by reverse transcription to cDNA using the Tetro cDNA Synthesis Kit (BIOLINE catalogue no. BIO-65050). This kit applies both Oligo dT

### 2.8. Prediction of mRNA secondary structure

RNA secondary structure regulates expression of many gene transcripts, and plays a substantial role in regulating transcription, splicing RNA, editing and transcript degradation and translation. RNA secondary structure is formed through hydrogen-bonding between pairs of complementary nucleotides in a transcript. In order to study the functional role of a transcript, it

suffices to know its RNA secondary structure [19]. All RNA folding tools calculate the minimum free energy (MFE) by adding up individual energy contributions from base pair stacking, bulges, hairpins, internal loops and multi-branch loops. The RNAfold server was selected for analysis, because it uses both the Wuchty algorithm and the McCaskill algorithm, which offers a wide variety of functions, having the benefit of computing all possible secondary structures within a narrow free-energy range [20,21]. This approach leads to the creation of one most likely structure. In contrast, some software servers predict secondary structures by calculating thermodynamics, e.g. UNAFold and RNA Structure use the Zuker algorithms to calculate the MFE and systematically sample structures within a percentage range of free-energy to create a set of diverse sub-optimal structures without providing a preference for the most likely outcome. Thus in this study, in order to predict the secondary structure of each hIFN $\gamma$  mRNAs, minimum free energy (MFE) structures and base pair probabilities from single RNA sequences, RNAfold WebServer (Vienna RNA Website) was used [20].

### 3. Results

#### 3.1. Confirmation of integration into *P. pastoris*

PCR products were amplified at the expected size for ~50 clones for all constructs using gene-specific forward and reverse primers. Amplification resulted in bands of the correct sizes of 0.5–1 kbp which was confirmed by sequence analysis at the AGRF demonstrating successful integration of the hIFN $\gamma$  gene into the yeast genome.

#### 3.2. SDS-PAGE & western blotting

Secretion of hIFN $\gamma$  in *P. pastoris* cultures was not detected using SDS-PAGE and anti-His Western blotting analysis. In contrast, expression of secreted positive control (P-Protein) was observed.

#### 3.3. ELISA

Low expression of secreted hIFN $\gamma$  was detected in some transformant cells of *P. pastoris* (Table 3), with highest levels found in CB7435-pPpT4 $\alpha$ S-COS2 and lowest in GS115-pPIC9-COS1, indicating that codon-optimisation of the sequence had no impact on expression yields. This was confirmed by non-detectable yields in the X33 strains transformed with the NS and COS2 sequences of hIFN $\gamma$ , respectively. As the latter results were also independent of vector used, this also indicates that expression of hIFN $\gamma$  was strain-dependent and affected by their resulting phenotype rather than the choice of vector and gene codon optimisation.

ELISA analysis of cell lysates of *P. pastoris* GS115-pPIC9-COS2 transformants demonstrated that hIFN $\gamma$  was successfully

secreted to medium (Table 3). GS115-pPIC9-COS2 transformant cells cultivated in unbuffered media yielded similar amounts of secreted hIFN $\gamma$  to those using buffered medium (Table 3) suggesting that extracellular proteolytic degradation of the product was not the cause of low yields. Despite the low expression, expression was enhanced 10-fold in using the codon-optimised sequence COS2 which had a lower MFE (GS115-pPIC9-COS2 in comparison to GS115-pPIC9-COS1 (Table 3) (Section 3.4.1).

#### 3.4. RNA analysis

##### 3.4.1. mRNA secondary structure

Although the secondary structures of mRNAs appeared to be different in bi-dimensional models, both codon-optimised sequences possessed similar predicted levels of the MFE compared to the natural sequence of hIFN $\gamma$ . Thus, a similar level of RNA stability would be expected (Fig. 3).

##### 3.4.2. Detection of hIFN $\gamma$ mRNA

Analysis of RT-qPCR result showed that approximately 2–3 copy number of hIFN $\gamma$  mRNA were found per cell (Table 4), which is considered as low abundance RNA.

### 4. Discussion

Codon preference between the recombinant gene and expression host has been established to be one bottleneck for protein translation in heterologous expression systems, hindering the translation of the recombinant gene transcript [22]. To overcome this potential problem, codon optimisation was used to adapt the foreign recombinant gene for successful and efficient heterologous expression in yeast systems [23]. Studies investigating the correlation between codon usage patterns and expression level for hIFN $\gamma$  proved that codon bias exists in CHO cells [3,22]. In contrast, our results did not show a significant impact on the expression of codon-optimised (COS1 & COS2) and non-codon-optimised, native (NS) sequences (Table 3). The potential for premature RNA truncation due to poly A signals in COS1 was refuted by proving that the poly A tail was in the correct location of the hIFN $\gamma$  mRNA using reverse transcription with the Oligo dT (18) primer and a primer pair binding close to the 5' end. This would suggest that RNA instability was not the cause of low expression. Moreover, analysis of the predicted secondary structures of mRNAs revealed more similar MFE levels of two sequences (NS, COS1) and slightly lower MFE level for the COS2 (Fig. 3) which could be the reason for enhancing the expression of the COS2 by 10 folds, this result is in conformity with previous reports indicating that manipulation of secondary structure of mRNA can effectively improve translation and heterologous expression of recombinant proteins in yeast [24].

**Table 3**  
Maximal yield of secreted hIFN $\gamma$  expressed in *P. pastoris* after 72 hpi (Mean  $\pm$  SD, n = 3).

Transformant (Strain-vector-sequence)	Phenotype	Material analysed	Max. yield ( $\mu$ g L $^{-1}$ )
<i>Pichia pastoris</i>	GS115-pPIC9-COS1	Supernatant/buffered	0.17 $\pm$ 0.02
	GS115-pPIC9-COS2	Supernatant/buffered	1.8 $\pm$ 0.06
		Cell lysate/buffered	0.4 $\pm$ 0.2
	X33-pPICZ $\alpha$ -NS	Supernatant/unbuffered	1 $\pm$ 0.2
		Supernatant/buffered	n.d.
	X33-pPICZ $\alpha$ -COS2	Supernatant/buffered	n.d.
	X33-pPpT4 $\alpha$ S-COS2	Supernatant/buffered	n.d.
	KM71H-pPICZ $\alpha$ -NS	Supernatant/buffered	12 $\pm$ 0.02
	KM71H-pPICZ $\alpha$ -COS2	Supernatant/buffered	9 $\pm$ 0.5
	CB7435-pPpT4 $\alpha$ S-COS2	Supernatant/buffered	16 $\pm$ 3

n.d.: not detected.

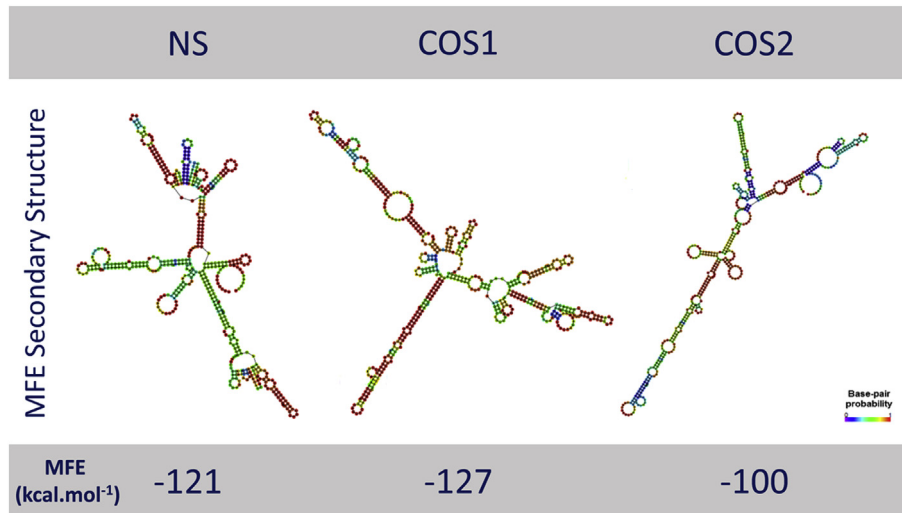


**Fig. 3.** Bi-dimensional modelling of mRNA secondary structure predicted based on the MFE. **NS:** Native sequence, **COS1:** Codon-optimised sequence 1, **COS2:** Codon-optimised sequence 2.

**Table 4**

*hIFN $\gamma$*  cDNA (= mRNA) copy number of GS115-pPIC9-COS1 *P. pastoris* transformants (Mean  $\pm$  SD, n = 3).

C(t)	14.4 $\pm$ 0.3
Initial copy number of <i>hIFN<math>\gamma</math></i> cDNA per volume reaction	43 $\times$ 10 <sup>3</sup> $\pm$ 7 $\times$ 10 <sup>3</sup>
Approx. <i>hIFN<math>\gamma</math></i> mRNA copy number per cell	2.6 $\pm$ 0.4

All transformants showed low to no expression of *hIFN $\gamma$* , however, an improvement of 100-fold was, achieved with transformants of the Mut<sup>S</sup> phenotype (Table 3). Several hypotheses can be formulated to explain this outcome.

1. The large difference in yields between Mut<sup>S</sup> and Mut<sup>+</sup> phenotypes could indicate that lack of the *AOX2* gene in the Mut<sup>S</sup> phenotype would result in higher yields. This raises the question whether the activity of *AOX2* interferes with transcription of *hIFN $\gamma$* . This hypothesis can be tested by using constitutive promoters in *P. pastoris* e.g. GAP promoter.

2. Undesired proteolysis of heterologous proteins expressed in *P. pastoris* and/or inefficient secretion could have caused lower product yields of the recombinant protein [11]. Proteolysis may occur in two ways; firstly, intracellularly, during vesicular transport of recombinant protein by secretory pathway-resident proteases and secondly extracellularly, by proteases being secreted or released into the culture medium [11]. For example, the yield of ovine interferon  $\tau$  decreased due to proteolysis and eventual degradation of the recombinant protein [25]. In contrast, our results render the low expression of *hIFN $\gamma$*  due to extracellular proteolytic activity and/or incomplete secretion unlikely. Furthermore, as the  $\alpha$ -mating factor secretion signal was incorporated into the design, neither addition nor deletion of the native secretion signal altered expression levels, as expected, and presence or absence of the His tag also had no impact.

3. A distinct possibility for the observed low expression in our study could be the low abundance of mRNA (estimated 2–3 copy numbers of *hIFN $\gamma$*  mRNA transcripts). To explain this, it needs to be noticed that a typical average cell contains ~10–30 pg total RNA composed of ~360,000 mRNA molecules. Low abundance mRNA species may have a copy number as low as 5–15 molecules per cell [26] This could be explained by assuming that either the *AOX* promoter was not activated to initiate transcription of *hIFN $\gamma$*  mRNA or induction of *AOX2* adversely impacted on transcription of *hIFN $\gamma$*  mRNA.

4. Intracellular degradation of the recombinant protein may be an additional cause for the low yields, which is supported by the apparent mismatch between anti-His Western blot detection and ELISA results which could have resulted in the removal of the His-tag prior to secretion. To examine this hypothesis, the use of protease-deficient strains of *P. pastoris* in future studies could be useful.

5. Protein mis-folding in the endoplasmic reticulum (ER) has been reported as one of the possible reasons for low production rates of proteins in yeast [13].

The *P. pastoris* expression system has only recently been investigated for the commercial production of *hIFN $\gamma$* , reporting secretion of around 300 mg L<sup>-1</sup> with a specific activity of 1  $\times$  10<sup>7</sup>–1.4  $\times$  10<sup>7</sup> IU mg<sup>-1</sup>, using the pPICZ $\alpha$  vector and the alcohol oxidase (*AOX1*) promoter [10]. Our yields of *hIFN $\gamma$*  were much lower and these outcomes were not improved using additional strains, vectors, codon-optimised sequences. In contrast to Wang, Ren [10], protein quantification was carried out in this study via ELISA instead of using the Bradford assay and purity-determination by HPLC. As we did not use the same restriction sites, it could be possible that KEX2 and/or STE13 cleavage was not efficient, leading to ineffective secretion, because the processing of the signal sequence of human interferon gamma occurs in two steps, firstly cleavage by KEX2 then STE13. Whilst we cannot exclude incomplete processing and secretion, our antibody detects the secreted protein, which would indicate that the antibody does not target the secretion signal sequence. In addition, we checked the cell lysate of GS115-pPIC9-COS2 and found that the protein was efficiently secreted with little remaining. We would therefore expect the same outcome for pPICZ, as we used the same cloning sites EcoRI/NotI. This, to our point of view, would suggest that the observed low yields are the result of more than just inefficient secretion, i.e. low mRNA copy numbers remain a highly likely reason.

Furthermore, the molecular weight of the unglycosylated recombinant *hIFN $\gamma$*  expressed in *E. coli* is 17.6 kDa; however, generally, the molecular weight of proteins increases due to glycosylation [27] Therefore, the expected molecular weight of *hIFN $\gamma$*  expressed in *P. pastoris* would be higher. The Western blot result, however, shown in Ref. [10] identified a 15 kDa band as *hIFN $\gamma$*  which is theoretically impossible unless the target protein was truncated and unglycosylated, which highlights the possibility of misidentification in the small-scale experiments. In contrast, the authors verified the nature of the secreted protein by N-terminal

sequencing following HPLC purification, suggesting that obtained yields might be achievable.

Comparison of the translated amino acid sequence shown in Ref. [10] (derived from the published optimised DNA sequence) to the native amino acid sequence of hIFN $\gamma$  revealed defects in three positions, *i.e.* there is a deletion of serine<sup>43</sup> and an addition of serine<sup>51</sup> and replacement of leucine<sup>50</sup> by phenylalanine<sup>50</sup> in the native polypeptide in the recombinant protein. While these differences may not impact on the determination of yields, it could alter the three-dimensional structure of the protein with potential impacts on biological activity.

Taken together, irrespective of sequence, vector and expression strain used, this study showed that the yield of hIFN $\gamma$  expressed in *P. pastoris* is too low for industrial-scale production. Similarly, a very recent study by Prabhu et al. (2016) also did not achieve high expression yields of hIFN $\gamma$  (<2.5 mg L<sup>-1</sup>), using a *P. pastoris* codon-optimised hIFN $\gamma$  sequence, the same strain of *P. pastoris* (GS115) and vector (pPICZ $\alpha$ ) under the control of AOX1 promoter, or a multiple copy number integration approach (pPIC9K, a multiple copy integrating vector) and process fermenter parameter optimisation, *viz.* agitation rate, inoculum size, methanol concentration, pH and temperature [13].

Although glycosylation of the protein by *P. pastoris* should lead to a longer half-life of the recombinant protein and higher biological activity, it needs to be considered that recombinant proteins can on occasions become over-glycosylated and content of high mannose glycans could cause immunogenicity in patients, which are two disadvantages of this expression system. Therefore, we recommend future studies to focus on improvement of expression of hIFN $\gamma$  in mammalian systems, as glycosylation patterns should be more similar to those found in human cells [3].

Among mammalian expression systems; CHO was the focal point of studies from the 1990s onward, achieving laboratory-scale secretion of 15 mg L<sup>-1</sup> of hIFN $\gamma$  [28] and studies included over-expression, optimisation of cultivation, scale-up production and purification [3,6,29,30]. An order of magnitude greater expression yields of hIFN $\gamma$  (570 mg mL<sup>-1</sup>) was achieved in mammary glands of transgenic mice *in vivo*, which is comparable to productivity in *E. coli* [7,31]. Studies in mammalian expression systems are ongoing to improve productivities further and to lower the cost of production, which is essential to make mammalian expression systems at the industrial scale competitive with the currently used *E. coli* expression system.

## 5. Conclusions

Around 50 transformant colonies of *P. pastoris* were screened for expression of hIFN $\gamma$  with yields ranging from not detectable to low. This was most likely the result of the low abundance of mRNA transcript and/or inefficient secretion. We, therefore, conclude that industrial production of hIFN $\gamma$  in *P. pastoris* is economically unrealistic, unless transcription/translation can be significantly increased. It is therefore recommended that commercial production focuses on other eukaryotic expression systems *e.g.* CHO, mammary gland expression in transgenic mice or even human embryonic kidney 293 (HEK293) cells. In addition, research has to focus on unravelling the cause of low expression of hIFN $\gamma$  in *P. pastoris* to overcome low yield hurdles to make the system competitive economically.

## Acknowledgments

We would like to thank Dr. Jose Domingos for providing some of the qPCR materials. KH acknowledges project support by the Advanced Manufacturing Cooperative Research Centre (AMCRC),

funded through the Australian Government's Cooperative Research Centre Scheme, grant number 2.3.4. The funders had no role in study design, data collection and analysis or preparation of the manuscript and have provided permission to publish. This research is part of the MBD Energy Research and Development programme for Biological Remediation of Methane from Underground Coal Mine Ventilation Air. Ali Razaghi was supported by an AMCRC Ph.D. scholarship.

## References

- [1] Marciano BE, Wesley Robert, Ellen S, Anderson Victoria L, Barnhart Lisa A, Darnell Dirk, et al. Long-term interferon- $\gamma$  therapy for patients with chronic granulomatous disease. *Clin Infect Dis* 2004;39:692–9.
- [2] Schroder K, Hertzog PJ, Ravasi T, Hume DA. Interferon-gamma: an overview of signals mechanisms and functions. *J Leukoc Biol* 2004;75:163–89.
- [3] Chung BK-S, Yusufi FN, Yang Y, Lee D-Y. Enhanced expression of codon optimized interferon gamma in CHO cells. *J Biotechnol* 2013;167:326–33.
- [4] Derynck R, Singh A, Goeddel DV. Expression of the human interferon- $\gamma$  cDNA in yeast. *Nucleic Acids Res* 1983;11:1819–37.
- [5] Chen WS, Villaflores OB, Jinn TR, Chan MT, Chang YC, Wu TY. Expression of recombinant human interferon-gamma with antiviral activity in the bi-cistronic baculovirus-insect/larval system. *Biosci Biotechnol Biochem* 2011;75:1342–8.
- [6] Fox SR, Patel UA, Yap MG, Wang DL. Maximizing interferon-gamma production by Chinese hamster ovary cells through temperature shift optimization: experimental and modeling. *Biotechnol Bioeng* 2004;85:177–84.
- [7] Bagis H, Aktoprakligil D, Gunes C, Arat S, Akkoc T, Cetinkaya G, et al. Expression of biologically active human interferon gamma in the milk of transgenic mice under the control of the murine whey acidic protein gene promoter. *Biochem Genet* 2011;49:251–7.
- [8] Nakajima T, Tsunoda S, Nakada S, Nagata S, Oda K. Hyperproduction of human interferon gamma by rat cells maintained in low-serum medium using the fibronectin gene promoter. *J Biochem* 1992;112:590–7.
- [9] Gray PW, Leung DW, Pennica D, Yelverton E, Najarian R, Simonsen CC, et al. Expression of human immune interferon cDNA in *E. coli* and monkey cells. *Nature* 1982;295:503–8.
- [10] Wang D, Ren H, Xu JW, Sun PD, Fang XD. Expression, purification and characterization of human interferon-gamma in *Pichia pastoris*. *Mol Med Rep* 2014;9:715–9.
- [11] Ahmad M, Hirz M, Pichler H, Schwab H. Protein expression in *Pichia pastoris*: recent achievements and perspectives for heterologous protein production. *Appl Microbiol Biotechnol* 2014;98:5301–17.
- [12] Pla A, Damasceno M, Vannelli T, Ritter G, Batt A, Shuler M. Evaluation of Mut<sup>+</sup> and Mut<sup>-</sup> *Pichia pastoris* phenotypes for high level extracellular scFv expression under feedback control of the methanol concentration. *Biotechnol Prog* 2006;22:881–8.
- [13] Prabhu AA, Veeranki VD, Dsilva SJ. Improving the production of human interferon gamma (hIFN- $\gamma$ ) in *Pichia pastoris* cell factory: an approach of cell level. *Process Biochem* 2016. <http://dx.doi.org/10.1016/j.procbio.2016.02.007>.
- [14] Näätsaari L, Mistlberger B, Ruth C, Hajek T, Hartner FS, Glieder A. Deletion of the *Pichia pastoris* KU70 homologue facilitates platform strain generation for gene expression and synthetic biology. *PLoS One* 2012;7:e39720.
- [15] Lin-Cereghino J, Wong WW, Giang W, Luong LT, Vu J, Johnson SD, et al. Condensed protocol for competent cell preparation and transformation of the methylotrophic yeast *Pichia pastoris*. *Biotechniques* 2005;38:44–8.
- [16] Razaghi A, Huerlimann R, Owens L, Heimann K. Increased expression and secretion of recombinant hIFN $\gamma$  through amino acid starvation-induced selective pressure on the adjacent *HIS4* gene in *Pichia pastoris*. *Acta Fac Pharm Univ Comen* 2015;62:43–50.
- [17] Nielsen J. *Metabolic engineering*. 1 ed. Springer Berlin Heidelberg; 2003.
- [18] Valencia Jiménez A, Wang H, Siegfried BD. Expression and characterization of a recombinant endoglucanase from western corn rootworm, in *Pichia pastoris*. *J Insect Sci* 2014;14:242.
- [19] Proctor JR, Meyer IM. CoFold: an RNA secondary structure prediction method that takes co-transcriptional folding into account. *Nucleic Acids Res* 2013;41:e102.
- [20] Gruber AR, Lorenz R, Bernhart SH, Neuböck R, Hofacker IL. The Vienna RNA Websuite. *Nucleic Acids Res* 2008;36:W70–W4.
- [21] Schroeder SJ. Advances in RNA structure prediction from sequence: new tools for generating hypotheses about viral RNA structure-function relationships. *J Virol* 2009;83:6326–34.
- [22] Gustafsson C, Govindarajan S, Minshull J. Codon bias and heterologous protein expression. *Trends Biotechnol* 2004;22:346–53.
- [23] Welch M, Villalobos A, Gustafsson C, Minshull J. You're one in a googol: optimizing genes for protein expression. *J R Soc Interface* 2009;6: S468–S76.
- [24] Gaspar P, Moura G, Santos MAS, Oliveira JL. mRNA secondary structure optimization using a correlated stem-loop prediction. *Nucleic Acids Res* 2013; 1–5.
- [25] Sinha J, Plantz BA, Inan M, Meagher MM. Causes of proteolytic degradation of secreted recombinant proteins produced in methylotrophic yeast *Pichia*



- pastoris*: case study with recombinant ovine interferon-tau. *Biotechnol Bioeng* 2005;89:102–12.
- [26] Alberts B, Johnson A, Lewis J, Morgan D, Raff M, Roberts K, et al. *Molecular biology of the cell*. 6th ed. New York Garland Publishing; 2014.
- [27] Moharir A, Peck SH, Budden T, Lee SY. The role of N-glycosylation in folding, trafficking, and functionality of lysosomal protein CLN5. *PLoS One* 2013;8:e74299.
- [28] McClain DA. Increasing IFN- $\gamma$  productivity in CHO cells through CDK inhibition. MITlibraries. Boston: Massachusetts Institute of Technology; 2010.
- [29] Mols J, Peeters-Joris C, Wattiez R, Agathos SN, Schneider Y-J. Recombinant interferon- $\gamma$  secreted by chinese hamster ovary-320 cells cultivated in suspension in protein-free media is protected against extracellular proteolysis by the expression of natural protease inhibitors and by the addition of plant protein hydrolysates to the culture medium. *In Vitro Cell Dev Biol Anim* 2005;41:83–91.
- [30] Pm C, Ap I, Pm H, At B. The macroheterogeneity of recombinant human interferon-gamma produced by Chinese-hamster ovary cells is affected by the protein and lipid content of the culture medium. *Biotechnol Appl Biochem* 1995;21:87–100.
- [31] Lagutin OV, Dobrovolsky VN, Vinogradova TV, Kyndiakov BN, Khodarovich YM, Jenkins N, et al. Efficient human IFN-gamma expression in the mammary gland of transgenic mice. *J Interferon Cytokine Res* 1999;19:137–44.